THE JOURNAL OF PHYSICAL CHEMISTRY A

Article

pubs.acs.org/JPCA

Uncovering the Terahertz Spectrum of Copper Sulfate Pentahydrate

Michael T. Ruggiero and Timothy M. Korter*

Department of Chemistry, Syracuse University, 1-014 Center for Science and Technology, Syracuse, New York 13244-4100, United States

ABSTRACT: Terahertz vibrational spectroscopy has evolved into a powerful tool for the detection and characterization of transition metal sulfate compounds, specifically for its ability to differentiate between various hydrated forms with high specificity. Copper(II) sulfate is one such system where multiple crystalline hydrates have had their terahertz spectra fully assigned, and the unique spectral fingerprints of the forms allows for characterization of multicomponent systems with relative ease. Yet the most commonly occurring form, copper(II) sulfate pentahydrate ($CuSO_4 \cdot 5H_2O$), has proven elusive due to the presence of a broad absorption across much of the terahertz region, making the unambiguous identification of its spectral signature difficult. Here, it is shown that the sub-100 cm^{-1} spectrum of $CuSO_4 \cdot 5H_2O$ is obscured by absorption from adsorbed water and that controlled drying reveals sharp underlying features. The crystalline composition of the samples was monitored in parallel by X-ray diffraction as a function of drying time, supporting the spectroscopic results. Finally, the terahertz spectrum of $CuSO_4 \cdot 5H_2O$ was fully assigned using solid-state density functional theory simulations, helping attribute the additional absorptions that appear after excessive drying to formation of $CuSO_4 \cdot 3H_2O$.

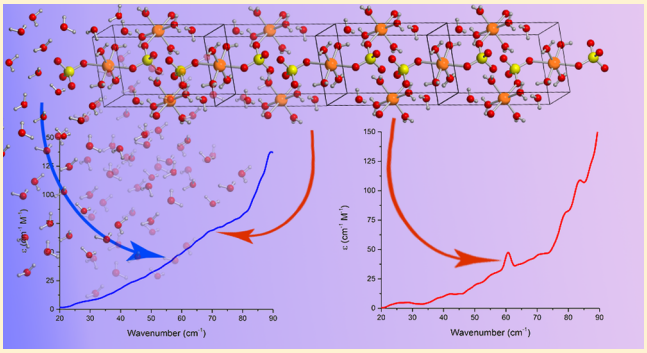

I. INTRODUCTION

Transition metal sulfates are common compounds with numerous applications.[1−5] These substances often contain varying levels of hydration, in terms of both cocrystallized and adsorbed water, which greatly alters the physical properties of the materials.[6,7] The extent of hydration is influenced by many factors with temperature and humidity being the most critical.[8−10] The dynamic nature of these effects often results in samples that have a mixture of several hydration states, making it difficult to determine the contributions of the different hydrated forms with great accuracy.[10−12] Terahertz (far-infrared) spectroscopy has proven to be a valuable analytical tool for characterizing hydration content not only because of its specific response to solid-state molecular arrangements and its nondestructive nature but also due to its sensitivity to bulk water content.[12−14] Recently, terahertz spectroscopy has been used to investigate various transition metal sulfates, and it was shown to provide detailed information that complemented other methods such as X-ray diffraction.[10,15] Because the low-frequency motions accessible by terahertz radiation are dependent on both internal and external structures, it provides a high level of reliability in detecting the presence of compounds that may be challenging to distinguish in the mid-infrared or even by diffraction methods.[16,17]

Terahertz spectroscopy of transition metal sulfates typically reveals well-resolved absorption features in the sub-100 cm^{-1} region.[10,15] Considering copper(II) sulfate specifically, terahertz spectra of anhydrous copper(II) sulfate and two of its three known hydrates (monohydrate and trihydrate) have had their spectral absorptions identified and assigned.[10,18] Unexpectedly, copper(II) sulfate pentahydrate ($CuSO_4 \cdot 5H_2O$) was found to deviate from the trend of the lower hydrates by exhibiting a broad rising absorption in the terahertz region with only very weak features possibly being resolved on top of this base. The broad and essentially featureless absorption spectrum of $CuSO_4 \cdot 5H_2O$ limits its analytical utility in terahertz spectroscopic sensing. This is unfortunate given that the pentahydrate is the most common copper(II) sulfate hydrate under typical conditions.[9,19] Complicating the analysis is that copper sulfate(II) is known to readily form mixed hydrate samples, and that the isolation of one particular form is difficult to achieve.[9,10] Thus, it is highly likely that a given sample of what may primarily be $CuSO_4 \cdot 5H_2O$ is actually contaminated by various hydrate species.

Solid-state density functional theory (DFT) calculations are an invaluable resource when studying multicomponent systems.[20−24] The simulation of the vibrational spectrum of each individual compound allows for qualitative spectral deconvolution of mixed samples.[21,23,25] In the case of anhydrous $CuSO_4$, the DFT results enabled the recognition that the "pure" sample actually contained detectable amounts of monohydrate and trihydrate species, which clearly altered the experimental terahertz spectrum.[10] Applying the same computational methods to $CuSO_4 \cdot 5H_2O$ enables the observed

Received: October 14, 2015
Revised: November 19, 2015
Published: January 5, 2016

DOI: 10.1021/acs.jpca.5b10063
J. Phys. Chem. A 2016, 120, 227−232

terahertz spectral results to be interpreted and reconciled with controlled dehydration experiments. Careful control of water content in the $CuSO_4 \cdot 5H_2O$ samples enables identification of the mechanisms responsible for the obscuring of its spectral signature. Ultimately, the combined experimental and theoretical results show that adsorbed surface water dominates the terahertz spectra of ambient condition samples, masking any discrete absorptions from the $CuSO_4 \cdot 5H_2O$ crystals.

II. METHODS

A. Experimental Section. Anhydrous $CuSO_4$ (Sigma-Aldrich, ≥ 99.99%) was fully dissolved in deionized water until the solution was deep blue in color. The aqueous mixture was placed in a standard laboratory fume hood for 1 week until all of the solvent evaporated. Large blue crystals of $CuSO_4 \cdot 5H_2O$ formed and were immediately prepared for experimental measurements by pulverizing in a stainless steel ball mill. The resultant blue powder was either used in that state or placed in a calcium sulfate (Drierite) desiccator in order to remove excess water.

To confirm bulk crystalline content, powder X-ray diffraction (PXRD) was always performed in parallel with the terahertz measurements. The pulverized samples were dispersed in paraben oil, mounted using a MiTeGen MicroMount, and placed under a stream of liquid nitrogen (to mimic the conditions of the single-crystal[26] and terahertz measurements). The PXRD data was obtained using a Bruker KAPPA APEX DUO diffractometer, which contains an APEX II CCD system, using monochromatic Cu Kα radiation (λ = 1.5418 Å). The experimental PXRD patterns were compared to patterns calculated from the experimental single-crystal[26] data using the Mercury[27] software.

Terahertz vibrational spectra were obtained from 20 to 90 cm^{-1} at both room (298 K) and liquid-nitrogen (78 K) temperatures with a time-domain pulsed spectrometer.[28] Zinc telluride crystals were used to generate and detect terahertz pulses through optical rectification[29,30] and free-space electro-optic sampling,[31] respectively. The spectrometer was continuously purged with dry air and the sample chamber held under vacuum in order to minimize absorption from atmospheric water. The samples were mixed with polytetrafluoroethylene (PTFE) and pressed into pellets with a final w/w concentration of ~2.5%. It is important to note that copper(II) sulfate is very hygroscopic and therefore sensitive to atmospheric water but once dispersed in the PTFE matrix and pressed into a pellet the samples were stable for at least 1 week. Terahertz time-domain waveforms were collected by averaging 32 scans over a 32 ps window and were subsequently Fourier transformed to create terahertz transmission spectra. Absorption units (ε, M^{-1} cm^{-1}, based on the concentration of crystallographic unit cells) were obtained by the division of a sample spectrum by a blank PTFE spectrum, and the presented spectra are a result of four averaged sample-blank data sets.

B. Theoretical. All solid-state DFT calculations were performed using the CRYSTAL14 software package.[32] On the basis of previous publications regarding metal-sulfate species,[10,15,26] the Becke-3-Lee–Yang–Parr (B3LYP)[33] density functional and the atom-centered 6-31G(d)/6-31G(2d,2p) basis sets[34] (copper/nonmetals) were used for the simulations. Geometry optimizations were initialized with experimentally determined atomic positions and were performed in the absence of any constraints other than the space group symmetry of the solid. Normal mode eigenvalues and eigenvectors were calculated from the optimized structure, using the central-difference numerical displacement method (two displacements per Cartesian axis, per atom). The infrared-active intensities were calculated using the Berry phase method.[35−37] The energy convergence criteria were set to $\Delta E < 10^{-8}$ and 10^{-10} hartree for the optimization and vibrational calculations, respectively.

III. RESULTS AND DISCUSSION

A. Terahertz Spectroscopy. *Initial Undried.* The PXRD pattern (Figure 1) of the initially prepared $CuSO_4 \cdot 5H_2O$ material showed that the sample contained pure $CuSO_4 \cdot 5H_2O$, and no reflections from any additional crystalline species were present. The terahertz spectrum of this sample (Figure 2a) was entirely featureless, only exhibiting broad absorption in the 20–90 cm^{-1} spectral range. This type of observed broad absorption has previously been shown to be caused by contamination from water that is not incorporated into the crystalline lattice but adsorbed to the particles.[13,15]

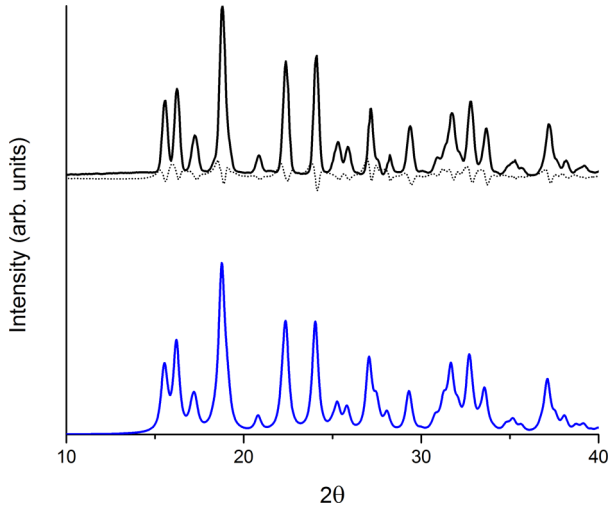

Figure 1. Experimental (black) and calculated (blue) PXRD patterns of $CuSO_4 \cdot 5H_2O$. The observed-minus-calculated residual is also shown (dotted trace).

Dried Six Hours. The $CuSO_4 \cdot 5H_2O$ powder was placed in a calcium sulfate desiccator for 6 h in order to gently remove excess water from the sample. The sample lost 2.58% of its original mass by the end of the drying period, but the PXRD pattern remained unchanged, indicating that only $CuSO_4 \cdot 5H_2O$ was present. It is important to note that the PXRD experiment accurately detects crystalline species present in samples but provides no information regarding the amount of disordered adsorbed water. The terahertz spectrum of the corresponding sample is presented in Figure 2b. Similar to the undried terahertz spectrum, the dried sample exhibits a significant absorption which begins at ~20 cm^{-1} and steadily increases beyond the spectral bandwidth of the instrument. However, upon drying, a resolvable absorption at 61.0 cm^{-1} appears with potential minor features between 75 and 90 cm^{-1} but still contains significantly fewer features than previously reported.[18] The unchanged PXRD pattern, yet altered terahertz spectra and significant mass loss, show that unincorporated water must be present in the $CuSO_4 \cdot 5H_2O$ samples when stored under normal conditions (which makes copper sulfate a functional

DOI: 10.1021/acs.jpca.5b10063
J. Phys. Chem. A 2016, 120, 227–232

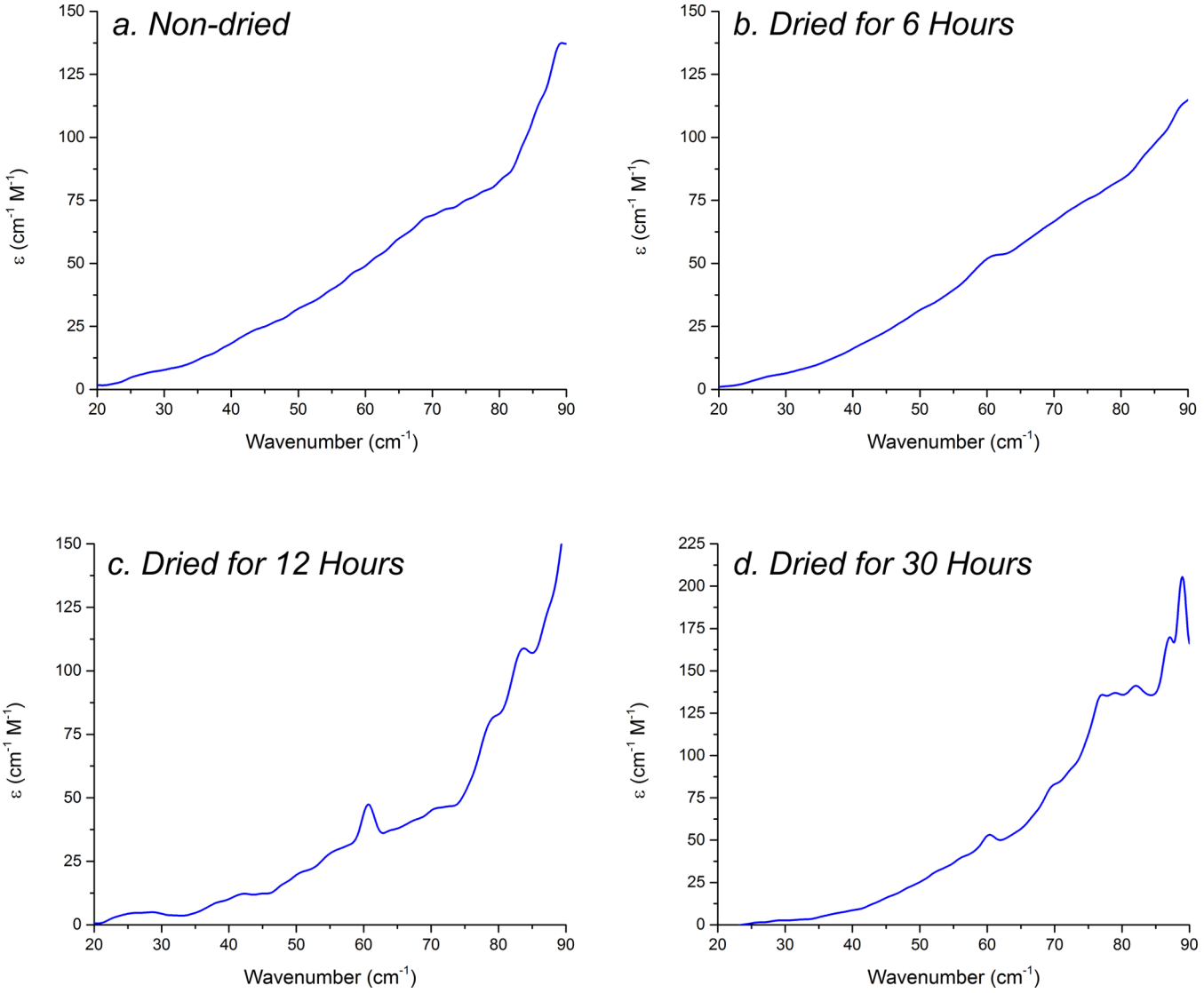

Figure 2. Terahertz spectra of $CuSO_4 \cdot 5H_2O$ after various drying intervals.

desiccant[38−40]) and highlights the sensitivity of terahertz spectroscopy to noncrystalline material.

Dried Twelve Hours. While the 6 h dried sample exhibited weak resolvable features, the terahertz spectrum still contained a broad absorption profile throughout the region, suggesting that unincorporated water was still present. The sample was placed into a desiccator for an additional 6 h, resulting in a cumulative mass loss of 5.46%. The PXRD pattern of the dried sample was again identical to the initial $CuSO_4 \cdot 5H_2O$ sample, indicating that no cocrystallized water was removed during the first 12 hours of drying. However, the terahertz spectrum changed considerably between 6 and 12 hours of drying with three additional features apparent at 71.4, 78.2, and 83.5 cm^{-1} (Figure 2c). Collectively, the changing terahertz spectrum, changing mass, but unchanged PXRD pattern further supports the hypothesis that the previously observed broad absorption originated from adsorbed water.

Dried Thirty Hours. In an attempt to remove any remaining adsorbed water, the sample was placed into the desiccator for an additional 18 h after which the sample now experienced a cumulative total mass loss of 6.80%. The PXRD pattern of the newly dried sample now contained additional reflections that could not be assigned to $CuSO_4 \cdot 5H_2O$, but matched the pattern of $CuSO_4 \cdot 3H_2O$ (Figure 3). The presence of additional crystalline species resulted in the appearance of at least two new terahertz absorptions (Figure 2d), occurring at 76.6 and 87.2 cm^{-1}. The frequencies of these features correlate with the previously published vibrational analysis of $CuSO_4 \cdot 3H_2O$[10], confirming the identity of the contaminant indicated in the PXRD measurement.

B. Theoretical Analysis. *Structural Details.* The experimental low-temperature single-crystal XRD structure of $CuSO_4 \cdot 5H_2O$ has already been detailed in the literature and will be discussed here only briefly.[26] Copper sulfate pentahydrate forms triclinic single crystals ($P\bar{1}$ space group symmetry) with lattice parameters of a = 6.106 Å, b = 10.656 Å, c = 5.969 Å, α = 77.332°, β = 82.433°, γ = 72.523°, and V = 360.548 $Å^3$ (Figure 4). The unit cell contains four formula units (Z = 4), and there are two symmetrically unique copper cations, resulting in two distinct coordination environments. The DFT geometry optimization accurately captures the internal and bulk structural details with low absolute errors (0.69% and 0.45% for bond and unit cell dimension errors,

DOI: 10.1021/acs.jpca.5b10063
J. Phys. Chem. A 2016, 120, 227−232

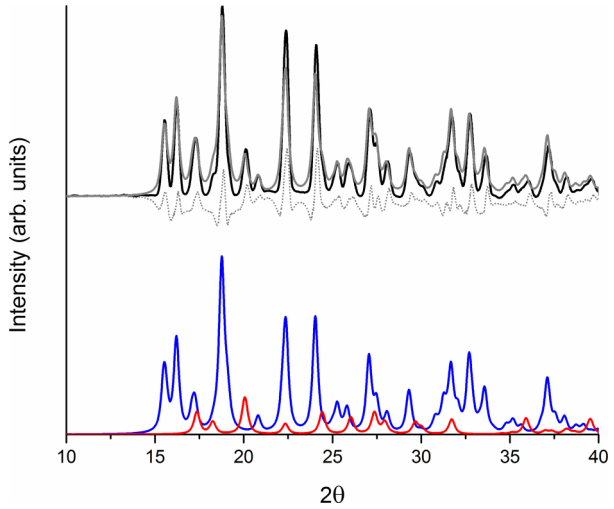

Figure 3. Dried (30 hours) PXRD pattern (black) of $CuSO_4{\cdot}5H_2O$. Contributions from $CuSO_4{\cdot}5H_2O$ (blue) and $CuSO_4{\cdot}3H_2O$ (red) are shown along with their summed pattern (gray) and observed-minus-calculated residual (dotted).

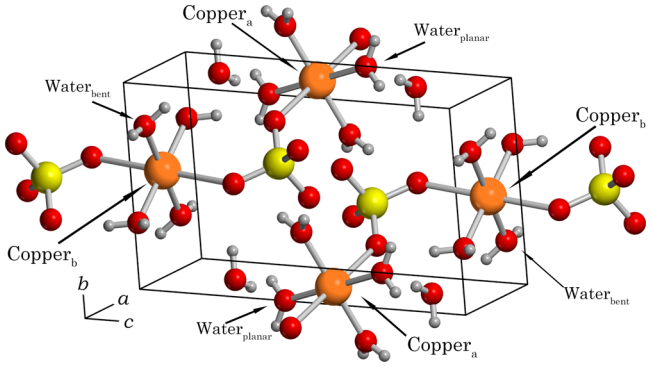

Figure 4. Fully optimized unit cell structure of $CuSO_4{\cdot}5H_2O$ with the referenced atoms labeled.

respectively). The high quality structural reproductions form the basis for vibrational simulations of the crystalline solids.

Vibrational Simulations. The variability of the experimental terahertz spectra with increasing drying times adds complexity to the definitive assignment of the absorption features. Solid-state DFT calculations provide the tools necessary to arrive at this information and help to elucidate the origins of the various absorptions in the $CuSO_4{\cdot}5H_2O$ terahertz spectra. The vibrational simulation shown in Figure 5 is in good agreement with the experimental spectrum, and the prediction of multiple intense modes above 90 cm^{-1} provides an explanation for the sharply rising absorption beginning near 75 cm^{-1}. The calculated spectrum was convolved using Lorentzian line shapes with the line width determined empirically from the experimental spectrum (fwhm = 3.3 cm^{-1}).

A full list describing the calculated normal modes and mode types is given in Table 1. All of the motions involve a significant amount of copper$_a$, copper$_b$, and water$_a$ motion with a small subset also containing water$_b$ motion. The motion of individual water molecules inside of the crystal lattice showcases the utility of terahertz spectroscopy in probing particular nonbonded interactions, interactions that would typically be inaccessible using traditional spectroscopic techniques.

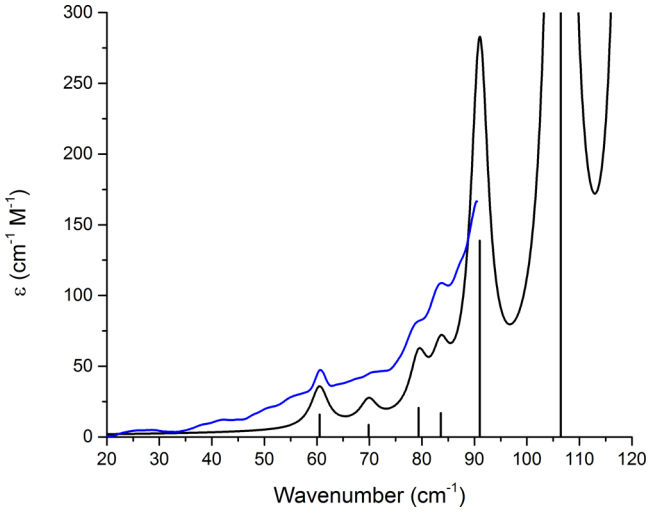

Figure 5. Twelve-hour dried terahertz spectrum of $CuSO_4{\cdot}5H_2O$ (blue) and solid-state simulated spectrum (black). The plot has been extended to 120 cm^{-1} to include the theoretically predicted modes outside of the experimental spectral bandwidth.

Table 1. Sub-120 cm^{-1} Vibrational Frequencies and Mode Types of Crystalline $CuSO_4{\cdot}5H_2O$

calculated frequency (cm^{-1})	experimental frequency (cm^{-1})	mode type
60.5	60.9	translation of copper cations with symmetric bending of each pair of water$_a$ (antisymmetric with respect to each other)
69.8	71.4	translation of copper cations with symmetric bending of one pair of water$_a$ molecules
79.3	78.2	translation of copper cations with water$_a$ umbrella motion and water$_{bent}$ scissor motion
83.5	83.5	rotation of water$_{planar}$ and sulfate-oxygens about the remaining water$_a$-copper$_a$ axis
91.0	90.8	antisymmetric translation of adjacent copper cations within the ribbon, with a copper$_a$-water$_a$ symmetric bend.
106.43	-	antisymmetric translation of adjacent copper cations within the ribbon, with a copper$_b$-water$_{bent}$ symmetric bend.

The complete assignment of the spectral features in the terahertz frequency range for $CuSO_4{\cdot}5H_2O$ confirms that the additional features in the 30 h dried sample are due to the production of an additional compound. The PXRD result (Figure 3) clearly showed the existence of $CuSO_4{\cdot}3H_2O$ and that data was used to determine the relative concentrations of the two materials. This was accomplished by taking linear combinations of the PXRD patterns of the two hydrates (obtained using the experimental single-crystal XRD structures) and subsequently minimizing the observed-minus-calculated residual. Each individual PXRD pattern was multiplied by an intensity scaling coefficient and the absolute value of the residual was optimized as a function of the two coefficients. This method produced an accurate reproduction of the experimental PXRD pattern with 24% of the sample found to be $CuSO_4{\cdot}3H_2O$, and the remainder being the pentahydrate. Conversion of this amount of $CuSO_4{\cdot}5H_2O$ to the trihydrate form corresponds to a mass loss of 3%, which is close to the measured value of 4% (mass loss between 12 and 30 h).

Scaling the simulated mode intensities by the appropriate population values yielded a combined $CuSO_4{\cdot}5H_2O$ and

DOI: 10.1021/acs.jpca.5b10063
J. Phys. Chem. A 2016, 120, 227−232

$CuSO_4·3H_2O$ terahertz spectrum (Figure 6), which is in good agreement with the experimental 30 h dried terahertz spectrum.

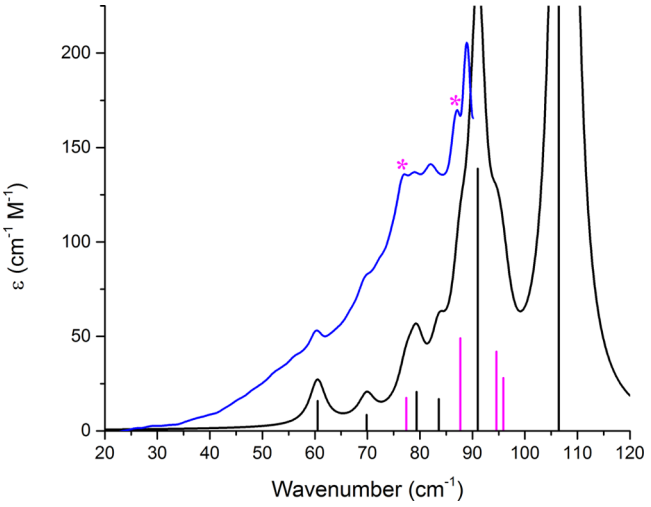

Figure 6. Thirty hour dried terahertz spectrum of $CuSO_4·5H_2O$ (blue) and simulated terahertz spectrum (purple) including contributions from both $CuSO_4·5H_2O$ (black sticks) and $CuSO_4·3H_2O$ (red sticks). Experimental trihydrate absorptions are marked with red asterisks (*). The line shape of the feature near 88.5 cm^{-1} is likely inaccurate since it occurs at the end of the instrument bandwidth.

Specifically, the two absorptions at 76.6 and 87.2 cm^{-1} that emerged after the prolonged drying period agree with the predicted $CuSO_4·3H_2O$ vibrational simulation.[10] While weak compared to the very strong absorption of $CuSO_4·5H_2O$, the inclusion of the $CuSO_4·3H_2O$ simulation helps to explain the significant differences between the 12 and 30 h spectra. The success of this binary fit helps highlight the use of terahertz spectroscopy as an analytical tool for the characterization of substances with mixed hydration states.

III. CONCLUSIONS

The terahertz spectrum of pure crystalline copper(II) sulfate pentahydrate was obtained and the spectral features fully assigned using solid-state density functional theory calculations. Initially, the $CuSO_4·5H_2O$ spectrum was obscured by a broad structureless absorption in the sub-100 cm^{-1} region. Through controlled drying and parallel powder X-ray diffraction measurements, the featureless absorption was unambiguously attributed to adsorbed water and not to crystalline hydrates. The experimental terahertz spectra and diffraction data were supported by the observed mass losses in the dried material. It was found that dehydration of $CuSO_4·5H_2O$ crystals must be done with great care, as the loss of cocrystallized water molecules is easily achieved by excessive drying times, resulting in the formation of the trihydrate species. The formation of $CuSO_4·3H_2O$ was revealed by diffraction methods and also resulted in the observation of new characteristic sharp absorption features in the terahertz spectrum of the sample. The results of this work demonstrate the sensitivity of terahertz spectroscopy to both cocrystallized and disordered water molecules and emphasize its use as an analytical probe of hydration levels in hygroscopic materials.

AUTHOR INFORMATION

Corresponding Author

*E-mail: tmkorter@syr.edu.

Notes

The authors declare no competing financial interest.

ACKNOWLEDGMENTS

This research was funded by a grant from the National Science Foundation (CHE-1301068). The authors thank Syracuse University for its continued support.

REFERENCES

(1) Walsh, W.; Morberg, P.; Yu, Y.; Yang, J. L.; Haggard, W.; Sheath, P.; Svehla, M.; Bruce, W. Response of a calcium sulfate bone graft substitute in a confined cancellous defect. *Clin. Orthop. Relat. Res.* **2003**, *406*, 228−236.

(2) Kelly, C. M.; Wilkins, R. M.; Gitelis, S.; Hartjen, C.; Watson, J. T.; Kim, P. T. The use of a surgical grade calcium sulfate as a bone graft substitute: results of a multicenter trial. *Clin. Orthop. Relat. Res.* **2001**, *382*, 42−50.

(3) Broughton, G. Calcium Sulfate Plasters. *Ind. Eng. Chem.* **1939**, *31*, 1002−1006.

(4) Kolar, J.; Štolfa, A.; Strlič, M.; Pompe, M.; Pihlar, B.; Budnar, M.; Simčič, J.; Reissland, B. Historical iron gall ink containing documents — Properties affecting their condition. *Anal. Chim. Acta* **2006**, *555*, 167−174.

(5) Salam, D.; El-Fadel, M. Mobility and availability of copper in agricultural soils irrigated from water treated with copper sulfate algaecide. *Water, Air, Soil Pollut.* **2008**, *195*, 3−13.

(6) Konsta-Gdoutos, M. S.; Shah, S. P. Hydration and properties of novel blended cements based on cement kiln dust and blast furnace slag. *Cem. Concr. Res.* **2003**, *33*, 1269−1276.

(7) Zhao, L.-J.; Zhang, Y.-H.; Wei, Z.-F.; Cheng, H.; Li, X.-H. Magnesium sulfate aerosols studied by FTIR spectroscopy: hygroscopic properties, supersaturated structures, and implications for seawater aerosols. *J. Phys. Chem. A* **2006**, *110*, 951−958.

(8) Wang, A.; Freeman, J. J.; Jolliff, B. L.; Chou, I.-M. Sulfates on Mars: A systematic Raman spectroscopic study of hydration states of magnesium sulfates. *Geochim. Cosmochim. Acta* **2006**, *70*, 6118−6135.

(9) Ting, V. P.; Henry, P. F.; Schmidtmann, M.; Wilson, C. C.; Weller, M. T. In situ neutron powder diffraction and structure determination in controlled humidities. *Chem. Commun.* **2009**, 7527−7529.

(10) Ruggiero, M. T.; Bardon, T.; Strlič, M.; Taday, P. F.; Korter, T. M. Assignment of the Terahertz Spectra of Crystalline Copper Sulfate and Its Hydrates via Solid-State Density Functional Theory. *J. Phys. Chem. A* **2014**, *118*, 10101−10108.

(11) Singh, R. S.; Tewari, P.; Bourges, J. L.; Hubschman, J. P.; Bennett, D. B.; Taylor, Z. D.; Lee, H.; Brown, E. R.; Grundfest, W. S.; Culjat, M. O. In *Terahertz sensing of corneal hydration*. Engineering in Medicine and Biology Society (EMBC), 2010 Annual International Conference of the IEEE, Aug. 31−Sept. 4, 2010; IEEE: Bellingham, WA, 2010; pp 3021−3024.

(12) Suen, J. Y.; Tewari, P.; Taylor, Z. D.; Grundfest, W. S.; Lee, H.; Brown, E. R.; Culjat, M. O.; Singh, R. S. Towards medical terahertz sensing of skin hydration. *Stud. Health Technol. Inform* **2009**, *142*, 364−368.

(13) Balakrishnan, J.; Fischer, B. M.; Abbott, D. Sensing the hygroscopicity of polymer and copolymer materials using terahertz time-domain spectroscopy. *Appl. Opt.* **2009**, *48*, 2262−2266.

(14) Heyden, M.; Ebbinghaus, S.; Havenith, M. Terahertz Spectroscopy as a Tool to Study Hydration Dynamics. In *Encyclopedia of Analytical Chemistry*; John Wiley & Sons, Ltd: New York, 2006.

(15) Ruggiero, M. T.; Bardon, T.; Strlic, M.; Taday, P. F.; Korter, T. M. The role of terahertz polariton absorption in the characterization of crystalline iron sulfate hydrates. *Phys. Chem. Chem. Phys.* **2015**, *17*, 9326.

DOI: 10.1021/acs.jpca.5b10063
J. Phys. Chem. A 2016, 120, 227−232

(16) Kawase, K.; Ogawa, Y.; Watanabe, Y.; Inoue, H. Non-destructive terahertz imaging of illicit drugs using spectral fingerprints. *Opt. Express* **2003**, *11*, 2549−2554.
(17) Ho, L.; Pepper, M.; Taday, P. Terahertz spectroscopy: Signatures and fingerprints. *Nat. Photonics* **2008**, *2*, 541−543.
(18) Fu, X.; Yang, G.; Sun, J.; Zhou, J. Vibrational Spectra of Copper Sulfate Hydrates Investigated with Low-Temperature Raman Spectroscopy and Terahertz Time Domain Spectroscopy. *J. Phys. Chem. A* **2012**, *116*, 7314−7318.
(19) Richardson, H. W. *Handbook of copper compounds and applications*; CRC Press: Boca Raton, FL, 1997.
(20) Chen, J.; Chen, Y.; Zhao, H.; Bastiaans, G. J.; Zhang, X.-C. Absorption coefficients of selected explosives and related compounds in the range of 0.1−2.8 THz. *Opt. Express* **2007**, *15*, 12060−12067.
(21) Strachan, C. J.; Taday, P. F.; Newnham, D. A.; Gordon, K. C.; Zeitler, J. A.; Pepper, M.; Rades, T. Using terahertz pulsed spectroscopy to quantify pharmaceutical polymorphism and crystallinity. *J. Pharm. Sci.* **2005**, *94*, 837−846.
(22) Zeitler, J. A.; Newnham, D. A.; Taday, P. F.; Threlfall, T. L.; Lancaster, R. W.; Berg, R. W.; Strachan, C. J.; Pepper, M.; Gordon, K. C.; Rades, T. Characterization of temperature-induced phase transitions in five polymorphic forms of sulfathiazole by terahertz pulsed spectroscopy and differential scanning calorimetry. *J. Pharm. Sci.* **2006**, *95*, 2486−2498.
(23) King, M. D.; Buchanan, W. D.; Korter, T. M. Identification and quantification of polymorphism in the pharmaceutical compound diclofenac acid by terahertz spectroscopy and solid-state density functional theory. *Anal. Chem.* **2011**, *83*, 3786−3792.
(24) Zeitler, J. A.; Taday, P. F.; Newnham, D. A.; Pepper, M.; Gordon, K. C.; Rades, T. Terahertz pulsed spectroscopy and imaging in the pharmaceutical setting-a review. *J. Pharm. Pharmacol.* **2007**, *59*, 209−223.
(25) Day, G. M.; Zeitler, J.; Jones, W.; Rades, T.; Taday, P. Understanding the influence of polymorphism on phonon spectra: lattice dynamics calculations and terahertz spectroscopy of carbamazepine. *J. Phys. Chem. B* **2006**, *110*, 447−456.
(26) Ruggiero, M. T.; Erba, A.; Orlando, R.; Korter, T. M. Origins of contrasting copper coordination geometries in crystalline copper sulfate pentahydrate. *Phys. Chem. Chem. Phys.* **2015**, *17*, 31023−31029.
(27) Macrae, C. F.; Bruno, I. J.; Chisholm, J. A.; Edgington, P. R.; McCabe, P.; Pidcock, E.; Rodriguez-Monge, L.; Taylor, R.; van de Streek, J.; Wood, P. A. Mercury CSD 2.0 - new features for the visualization and investigation of crystal structures. *J. Appl. Crystallogr.* **2008**, *41*, 466−470.
(28) Hakey, P. M.; Allis, D. G.; Ouellette, W.; Korter, T. M. Cryogenic terahertz spectrum of (+)-methamphetamine hydrochloride and assignment using solid-state density functional theory. *J. Phys. Chem. A* **2009**, *113*, 5119−5127.
(29) Rice, A.; Jin, Y.; Ma, X. F.; Zhang, X. C.; Bliss, D.; Larkin, J.; Alexander, M. Terahertz optical rectification from ⟨110⟩ zinc-blende crystals. *Appl. Phys. Lett.* **1994**, *64*, 1324−1326.
(30) Zhang, X. C.; Ma, X. F.; Jin, Y.; Lu, T. M.; Boden, E. P.; Phelps, P. D.; Stewart, K. R.; Yakymyshyn, C. P. Terahertz optical rectification from a nonlinear organic crystal. *Appl. Phys. Lett.* **1992**, *61*, 3080−3082.
(31) Wu, Q.; Litz, M.; Zhang, X. C. Broadband detection capability of ZnTe electro-optic field detectors. *Appl. Phys. Lett.* **1996**, *68*, 2924.
(32) Dovesi, R.; et al. CRYSTAL14: A program for the ab initio investigation of crystalline solids. *Int. J. Quantum Chem.* **2014**, *114*, 1287−1317.
(33) Becke, A. D. Density-functional thermochemistry. III. The role of exact exchange. *J. Chem. Phys.* **1993**, *98*, 5648−5652.
(34) Krishnan, R.; Binkley, J. S.; Seeger, R.; Pople, J. A. Self-consistent molecular orbital methods. XX. A basis set for correlated wave functions. *J. Chem. Phys.* **1980**, *72*, 650−654.
(35) Pascale, F.; Zicovich-Wilson, C. M.; López Gejo, F.; Civalleri, B.; Orlando, R.; Dovesi, R. The calculation of the vibrational frequencies of crystalline compounds and its implementation in the CRYSTAL code. *J. Comput. Chem.* **2004**, *25*, 888−897.
(36) Zicovich-Wilson, C. M.; Pascale, F.; Roetti, C.; Saunders, V. R.; Orlando, R.; Dovesi, R. Calculation of the vibration frequencies of α-quartz: The effect of Hamiltonian and basis set. *J. Comput. Chem.* **2004**, *25*, 1873−1881.
(37) Noel, Y.; Zicovich-Wilson, C. M.; Civalleri, B.; D'Arco, P.; Dovesi, R. Polarization properties of ZnO and BeO: An *ab initio* study through the Berry phase and Wannier functions approaches. *Phys. Rev. B: Condens. Matter Mater. Phys.* **2001**, *65*, 014111.
(38) Dover, M. V.; Marden, J. W. A Comparison of The Efficiency of Some Common Desiccants. *J. Am. Chem. Soc.* **1917**, *39*, 1609−1614.
(39) Trusell, F.; Diehl, H. Efficiency of Chemical Desiccants. *Anal. Chem.* **1963**, *35*, 674−677.
(40) Burfield, D. R.; Smithers, R. H. Desiccant efficiency in solvent drying. 3. Dipolar aprotic solvents. *J. Org. Chem.* **1978**, *43*, 3966−3968.

DOI: 10.1021/acs.jpca.5b10063
J. Phys. Chem. A 2016, 120, 227−232